tide-binding groove. The specific residues were α18 to α26, α29 to α34, β24 to β32, and β37 to β42.
23. The crystal structures of I-A^d (*15*) complexed with peptides $OVA_{323-339}$ [Protein Data Bank (PDB) code 1IAO] or $HA_{126-138}$ (PDB code 2IAD) were each superimposed onto I-A^{g7} (*22*); both gave the same rmsd value to two significant figures.
24. D. H. Fremont *et al.*, *Immunity* **8**, 305 (1998).
25. This displacement actually encompasses $Ala^{\beta49}$ to $Ala^{\beta58}$, which contribute to part of the S4 β-strand, a connecting loop segment, and the start of the H1 α-helix. Maximum rms deviations between I-A^{g7} and I-A^d within this region are around residues β55 to β57. The C_α-C_α distances between the equivalent β55 to β57 residues in I-A^{g7} and I-A^d-$HA_{126-138}$ are 1.29, 1.76, and 1.19 Å, respectively.
26. $Tyr^{\beta61}$ is positioned near the end of the H1 α-helical segment, and its side chain forms part of the wall of the peptide-binding groove. Although the $Tyr^{\beta61}$ side chain of I-A^{g7} overlaps spatially with the corresponding residue $Trp^{\beta61}$ in I-A^d and I-A^k, differences (70° to 79°) in the torsion angle χ_2 resulted in the planes of the aromatic side chains being almost perpendicular to each other (Fig. 2C). Accommodation of the increased volume resulting from the side chain of $Tyr^{\beta61}$, parallel to the α helix of the domain, was achieved by displacement of the region $Ala^{\beta49}$ to $Ala^{\beta58}$. $His^{\beta9}$ in the S1 β-strand forms part of the floor of the peptide groove, and its side chain in I-A^{g7} only subtly perturbs the surrounding region when compared with I-A^d. However, movement of the I-A^{g7} $Tyr^{\beta37}$ side chain (by ~15° around χ_1), relative to I-A^d, allowed for the larger side chain of $His^{\beta9}$. A domino effect was seen in I-A^{g7} because movement of the $Tyr^{\beta37}$ side chain had itself to be accommodated. Displacement of the region $Leu^{\beta53}$ to $Ser^{\beta57}$ outward might, therefore, be due in part to the polymorphic residue $His^{\beta9}$.
27. E. A. Nalefski, K. T. Shaw, A. Rao, *J. Biol. Chem.* **270**, 22351 (1995).
28. A plot of the average B_{value} for each residue of the peptide showed minimal relative mobility. Minima occurred near the center of the peptide (P4 to P6), whereas maxima occurred at the COOH-terminus. These differences were completely consistent with those observed in I-A^d and I-A^k and were therefore not significant.
29. First, residue $Asn^{\alpha69}$ does not form a bidentate hydrogen bond with P7, as seen in most class II structures; instead, the P7 carbonyl oxygen hydrogen bonds to the side-chain hydroxyl of $Tyr^{\beta61}$. Also, the P8 carbonyl oxygen no longer hydrogen bonds with residue β61 owing to the absence of Trp at this position, but forms a substitute hydrogen bond with the hydroxyl of polymorphic residue $Tyr^{\beta66}$. This polymorphic position corresponds to the site of a two-residue deletion between the helical segments H1 and H2a, when compared with I-A^d, and leads to a rearrangement of the standard hydrogen bonding pattern with the P7 and P8 residues.
30. No hydrogen bonds with good geometry are made between these two residues.
31. D. H. Hausmann *et al.*, *J. Exp. Med.* **189**, 1723 (1999).
32. The $Pro^{\beta56}$ side chain creates an overhang (Fig. 2C) that buries a large part of the $Arg^{\alpha76}$ side chain. Substitution by $His^{\beta56}$ makes the side chain of $Arg^{\alpha76}$ much more accessible but does not directly destabilize the H1 segment of the β1 because its main-chain conformation and the adjacent residues are similar to that of I-A^d and I-A^k.
33. For HLA-DR1, position β56 is a putative contact for the coreceptor CD4 [J. Brogdon *et al.*, *J. Immunol.* **161**, 5472 (1998)]; the presence of $His^{\beta56}$, in I-A^{g7}, instead of the usual $Pro^{\beta56}$ could alter the type of signal transmitted to the $CD4^+$ T cell.
34. D. L. Kaufman *et al.*, *Nature* **366**, 69 (1993).
35. B. Reizis *et al.*, *Int. Immunol.* **9**, 43 (1997).
36. K. Bartnes *et al.*, *Int. Immunol.* **9**, 1185 (1997).
37. G. Y. Liu *et al.*, *Immunogenetics* **37**, 296 (1993).
38. C. Stiffel *et al.*, *Immunol. Lett.* **16**, 205 (1987).
39. A. L. Corper, L. Teyton, I. A. Wilson, unpublished data.
40. L. C. Harrison *et al.*, *J. Exp. Med.* **185**, 1013 (1997).
41. Biosym Technologies, San Diego, CA, USA.
42. E. A. Stura and I. A. Wilson, *J. Crystal Growth* **110**, 270 (1991).
43. Z. Otwinowski and W. Minor, *Methods Enzymol.* **276**, 307 (1997).
44. B. W. Matthews, *J. Mol. Biol.* **33**, 491 (1968).
45. CCP4, *Acta Crystallogr. D* **50**, 760 (1994).
46. J. Navaza, *Acta Crystallogr. A* **50**, 157 (1994).
47. A. T. Brünger *et al.*, *Acta Crystallogr. D* **54**, 905 (1998).
48. R. J. Read, *Methods Enzymol.* **277**, 110 (1997).
49. T. A. Jones, J. Y. Zou, S. W. Cowan, Kjeldgaard, *Acta Crystallogr. A* **47**, 110 (1991).
50. A. T. Brünger, *Nature* **355**, 472 (1992).
51. The final structure contains 3012 protein atoms, 76 solvent molecules, and no carbohydrate. The following residues were built for I-A^{g7}–$GAD_{207-220}$: α1B to α178, α1S to α2S, β5 to β104, β113 to β188, β1S and β207P to β220P. Density for the loop β105 to β112 was absent and was therefore not built. Side-chain density for the following residues was absent and was therefore truncated back to the C_β atom: $Asp^{\alpha18}$, $Lys^{\alpha40}$, $Lys^{\beta63}$, $Glu^{\beta85}$, $Asn^{\beta113}$, $His^{\beta166}$, $Tyr_{\beta207P}$, $Tyr_{\beta218P}$, and $Thr_{\beta220P}$. Residues α1S, α2S, and β1S are the remains of the spacer(s), whereas β207P to β220P is the tethered GAD peptide.
52. R. A. Laskowski *et al.*, *J. Appl. Crystallogr.* **26**, 283 (1993).
53. D. E. Smilek, C. B. Lock, H. O. McDevitt, *Immunol. Rev.* **118**, 37 (1990).
54. D. Daniel and D. R. Wegmann, *Proc. Natl. Acad. Sci. U.S.A.* **93**, 956 (1996).
55. D. Elias *et al.*, *Proc. Natl. Acad. Sci. U.S.A.* **88**, 3088 (1991).
56. E. Carrasco-Marin, O. Kanagawa, E. R. Unanue, *Proc. Natl. Acad. Sci. U.S.A.* **96**, 8621 (1999).
57. U. Hurtenbach *et al.*, *J. Exp. Med.* **177**, 1499 (1993).
58. S. Amor *et al.*, *J. Immunol.* **150**, 5666 (1993).
59. NH_2-terminal Edmann degradation of the β chain of I-A^{g7} was carried out in order to confirm the GAD_{207} sequence. The 19 residues that were sequenced (gsh-srgYEIAPVFVLLEYV) correspond to part of the signal peptide (lowercase) and the correct sequence for $GAD_{207-219}$.
60. T. S. Jardetzky *et al.*, *Nature* **368**, 711 (1994).
61. K. J. Smith *et al.*, *J. Exp. Med.* **188**, 1511 (1998).
62. A. Dessen *et al.*, *Immunity* **7**, 473 (1997).
63. I. K. McDonald and J. M. Thornton, *J. Mol. Biol.* **238**, 777 (1994).
64. Calculated within the Viewer module of Insight II (*41*). Extended VDW radii were used.
65. We thank the staff at SSRL beamline 7-1, and H. McDevitt, D. Fremont, H. Grey, M. Taussig, and D. Williams for helpful discussions. Special thanks to N. Sarvetnick for the GAD65 peptide library, to A. Lehuen and J. Fehling for providing the cDNAs for I-A^{g7} β and GAD65, and to R. Stanfield for data collection and analysis. Supported by NIH grants CA58896 (I.A.W.) and DK55037 (L.T.) and by a National Health and Medical Research Council of Australia. C. J. Martin Fellowship (V.A.). This is publication 13001-MB from the Scripps Research Institute. The coordinates and structure factors for I-A^{g7}–$GAD_{207-220}$ have been deposited without hold in the PDB (access code 1ES0) and are available immediately from wilson@scripps.edu

4 February 2000; accepted 28 March 2000

The Eye Injury of King Philip II and the Skeletal Evidence from the Royal Tomb II at Vergina

Antonis Bartsiokas

The Royal Tomb II was discovered in Vergina, Greece, in 1977. It contained a male skeleton and a rich array of grave goods. Evidence of trauma supposedly in the orbital bones of the skull has been thought to correspond to an eye injury that King Philip II is historically known to have suffered. However, reexamination of the orbital morphology showed no evidence of such pathology. Therefore, the skeleton does not belong to Philip II. New skeletal evidence shows that the skeleton belongs to King Philip III Arrhidaeus. In this case, the tomb may well contain some of the paraphernalia of Alexander the Great.

A tomb designated Royal Tomb II was discovered at Vergina by Andronicos in 1977 (*1*). It was divided into two chambers. The main chamber contained a marble sarcophagus inside of which a golden chest (or larnax) bearing the Macedonian star burst was discovered. The chest contained the almost complete cremated skeleton of a man. Within the antechamber, a similar sarcophagus and chest were discovered, containing the cremated skeleton of a woman. The richness of the grave goods was astonishing. Among them, two small ivory heads have been identified as those of King Philip II and Alexander the Great (*1*). There were also a gilded silver diadem, a gold-sheathed sceptre, an iron and gold cuirass, an iron helmet, and an elaborate ceremonial shield (*1*). Considerable interest has been focused on the identification of the male occupant of the tomb. Andronicos, on the basis of archaeological evidence that pointed to a date around 336 B.C., identified the tomb as that of King Philip II of Macedon (*1*), father of Alexander the Great. However, mounting archaeological evidence (*2*, *3*) that points to a date around 317 B.C. suggests that the tomb belongs to King Philip III Arrhidaeus, son of Philip II and half-brother of Alexander the Great. As a result, the anthropological evidence became crucial to test the archaeological hypotheses.

The aim here is to study the paleopathology of the male skeleton using macrophotography, because no close-up pictures of his injuries had ever been obtained to study the microstructure of the wounds. Macropho-

Anaximandrian Institute of Human Evolution, 6 Aeginis Street, GR-166 73 Voula, Greece. E-mail: anaxbart@otenet.gr

tography was used for all points of facial anatomy at issue (Figs. 1 through 4). This method provided the proper magnification, often termed "natural size" (1:1) among photographers; that is, that obtained between a microscope lens and a normal camera lens. As a result, the whole structure under study was included in the photograph, and the necessary depth of field was obtained. Here, for instance, the magnification obtained in Fig. 1, with a Minolta 700si camera and a macro lens, is ×4. It could have been much more if needed. Fujichrome Sensia film rated at 100 was used at an f-stop of 32 and a shutter speed of 1/60 s in all close-up pictures. This method is simple, fast, and portable, but it requires some skill in photography. With microscopy, it is difficult to obtain such a low magnification with such a high depth of field. I examined the male skeleton from Royal Tomb II in the laboratories of the Vergina Archaeological Museum in 1998. The bones were in excellent condition because they were consolidated and restored quite satisfactorily (wherever that was possible) by Xirotiris before 1981 (*4*).

The bone pathology of the male skeleton is crucial as to the identification of the occupant of Royal Tomb II, because it is historically known that Philip II, being a warrior, suffered many wounds (*5*); whereas Arrhidaeus, being unwarlike, suffered none (*1, 6*). These wounds of Philip II would undoubtedly have left their mark on his skeleton. For instance, his right clavicle was shattered with a lance in 345 or 344 B.C., a wound to his right femur was nearly fatal and left Philip II lame 3 years before his death, and another wound maimed his arm (*5*). The most important of his wounds is the blinding wound Philip II suffered to his right eye from an arrow at the siege of Methone in 354 B.C., 18 years before he was assassinated in 336 B.C. (*5*).

In a thorough investigation, including the use of radiography and histology, Xirotiris and Langenscheidt found no evidence of any postcranial injuries, only slight degenerative changes (*4*) that were apparently the effect of osteoarthritis. Similarly, Prag and Neave agree that there is no evidence of any fresh or healed damage to the postcranial skeleton (*7*), an observation that is confirmed here as well. The only wound previously reported on the skeleton of the male occupant of Royal Tomb II was an eye injury to the skull (*6, 8*). This injury has become the hallmark of the identification of the male occupant of Royal Tomb II as Philip II (*7*) and has led to a famous reconstruction of his face showing a scar over his right eye (*8*). The original report found no morphological or radiographic evidence of any injury to the skull that was consistent with the severe eye wound suffered by Philip II (*4*). It was concluded that the hypothesis that Philip II and his wife Cleopatra were the occupants of Royal Tomb II was supported only by the age and sex determinations of the human remains (*4*). In view of the similar biological ages of Arrhidaeus and his wife Eurydice, the age determinations are no longer conclusive for the identification of the occupants of Royal Tomb II (*2, 6*). Others (*6*), however, reported that there is a "notch" on the superior margin of the right orbit, supposedly made by the arrow that injured Philip II (Figs. 1 and 2). It was also reported that there is a "pimple" of bone close to where the supraorbital nerve would have passed; this was cited as evidence of healing after the injury (*6*) (Figs. 1 and 2). In this way, the alleged eye injury to the skull (*8*) provided the identification for the occupants of Royal Tomb II (*5*).

I studied the anatomy of the right orbit of the male skull of Royal Tomb II (Figs. 1 and 2) by means of macrophotography. As seen in Figs. 1 and 2 of the right orbit, the "pimple" anatomically corresponds to the bony protuberance of the supraorbital notch and therefore does not constitute evidence of bone remodeling or callus formation. This bony protuberance is even less pronounced than those of many recent nonpathologic skulls (*9*). There is some surface roughening over the bony protuberance, but there is more roughening on the left orbit. Similarly, the "notch" is identified with what is anatomically termed the frontal notch (Figs. 1 and 2) and bears no evidence of healing or callus formation as would be expected in a notch made by an arrowhead. The evidence provided here regarding the right orbit may explain the discrepancy in which the famous reconstruction of the eye scar (*8*) shows a nick in the right eyebrow (presumably made by the descending arrow) running in direction from the upper left to the lower right (/), whereas the small ivory head of King Philip II used by the advocates of a Philip II identification (*1*) shows the brow nick running in the opposite direction (\). It has been suggested that there is an abnormal asymmetry between the two orbits of the frontal bone that is caused mainly by the notch (*6*). However, a fracture line that runs parallel to the supraorbital margin of the left orbit shows that the bone was lifted up during cremation, so as to create this seeming asymmetry (Fig. 4). Regardless of the cremation effects, it is not unusual to have a supraorbital notch on the right orbit and a supraorbital foramen on the left orbit of the same skull, resulting in a normal asymmetry between the two orbits (*10*).

It has been reported that the male skull presents a facial asymmetry that is the result of the arrow wound that removed Philip's right eye (*11*). Since there is no skeletal evidence of such an arrow wound, as has been shown here, it follows that there is no facial asymmetry (at least caused by such an arrow wound) either. Besides, there is no reason why such a facial wound would result in such an extensive bone remodeling that would change the whole symmetry of the face. At the most, it would cause a bone reaction to a possible infection. But no such infection is evidenced by the skull. There has also been mention of a "healed fracture" (*6,*

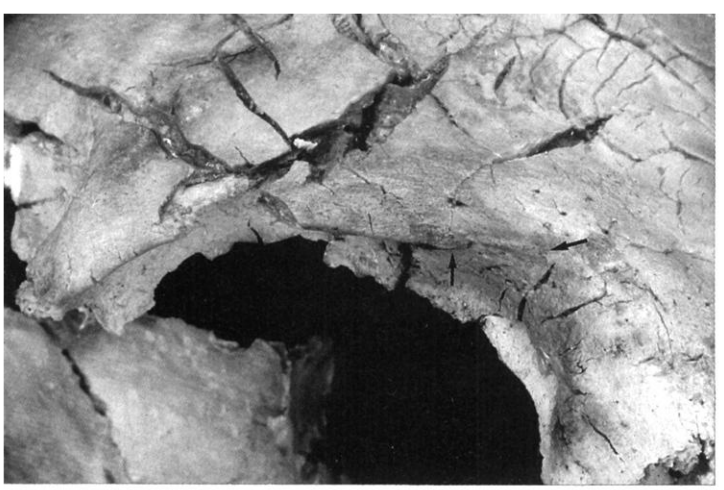

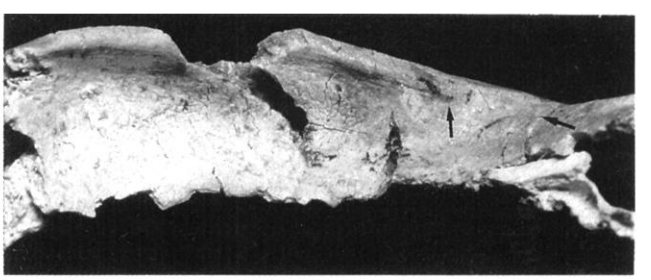

Fig. 1 (left). The right orbital margin of the male occupant of Royal Tomb II at Vergina (frontal view). The left arrow shows the bony protuberance of the supraorbital notch, and the right arrow shows the frontal notch. No evidence of healing or callus formation can be observed. **Fig. 2 (right).** The right orbital margin of the male occupant of Royal Tomb II at Vergina (internal view). The left arrow shows the bony protuberance of the supraorbital notch, and the right arrow shows the frontal notch. No evidence of healing or callus formation can be observed.

7) at the zygomaticomaxillary suture caused by the arrow, which after hitting the eye "struck the cheekbone at the join between the maxilla and the zygomaxillare with such force that it caused the suture to open and the two bones to move out of alignment. A small piece of bone was knocked away in the incident" (*7*). Again, there is no evidence of healing at this suture (Fig. 3), because the trabecular bone is still exposed, apparently from a crack made during cremation. If it were healed, no trabecular would be exposed because 18 years had passed between the wound and Philip's II death. The suggested antemortem fracture in this area is an artifact of the skull reconstruction (*12*). What the skull shows is bone distortion owing partly to cremation and partly to a poor reconstruction of the facial skeleton. In other words, we conclude that the "healed fracture" is an artifact of whatever these bones suffered postmortem. Similarly, the reported gross asymmetry between the lateral walls of the right and left maxillary sinuses (*7, 13*) is a result of this poor reconstruction (Fig. 3). A fragment of the jugal crest was broken off, apparently during cremation, and then badly reconstructed so as to give the impression of asymmetry. The presence of "osteophytes" (*13*) (apparently meaning exostosis) and alveolar resorption on the right side of the alveolar process (*11, 13*) as a result of possible periodontal disease is too limited (*4*) to account for the seeming asymmetry. Regarding the state of preservation in the area of the "nick," there is no difference between what Xirotiris in 1981, Musgrave in 1983, and myself in 1998 studied, as can be seen from the photographs they produced (*4, 6*). Thus, the material examined by Musgrave and myself was not less complete or in any way downgraded since Xirotiris reconstructed it, refuting any suggestion that differing things were examined.

It should be noted that the direction of the "notch" in the orbit is different from the position of the supposed "healed fracture" of the cheek; the "notch" goes straight into the orbit, whereas the supposed "healed fracture" is in a completely different level and direction. The arrow could not have knocked away a piece of bone from the zygomaticomaxillary suture had it not first struck the infraorbital margin, because the former is tucked under the latter. However, no evidence of such injury in the infraorbital margin exists. The suggested asymmetry of the mandible (*6, 7*) is also the result of cremation and not the result of congenital deformation or injury; the mandible, for instance, is wider than the maxilla. Bone is very pliable when on fire. Therefore, bones in cremations may easily be deformed by the weight of overlying items, such as burning wood. Experiments in kilns and ovens can be misleading [see, for example (*7, 13*)]. In such experiments, the bones are placed on flat surfaces and remain rather undistorted without the effect of any overlying weight.

For various archaeological and historical reasons (*1, 6, 14*), it is unlikely that Arrhidaeus was cremated soon after death: It has been suggested that after Arrhidaeus' assassination and burial by Olympias in 317 B.C., Cassander exhumed, cremated, and reburied Arrhidaeus the following year; that is, about 6 months after his death. It seems that Cassander did that as a policy to establish his own legitimacy by honoring the last king of the Argeads. So the critical question that would determine the identity of the cremains is whether there is any way of determining from the bones themselves whether they were cremated with flesh around them or cremated dry (degreased) after the flesh had been decomposed by burial. Fortunately, forensic anthropology can give the answer: Long bones cremated dry are nearly intact in size and form and show negligible warping; they assume a light brown color and present infrequent and straight transverse fractures (*15*). Long bones cremated fleshed are fragmentary with marked warping; they assume a white, blue, and gray color and present frequent and parallel-sided transverse fractures that are either curved (thumbnail) or serrated (*15*) (it is not as yet clear what happens to the flat bones). In flesh-covered bones, the mechanical alterations mentioned above occur because of the denaturation and contraction of bone collagen at high temperatures (*16*). This produces many transverse cracks perpendicular to the direction of the collagen fibers (that is, the long axis of the bone) and marked warping as the collagen contraction drags the bone mineral along. If the bone is dry because of having been buried in the ground, the collagen-apatite bonds weaken (*17*) and the collagen is hydrolyzed into smaller peptide products (*18*). Then, during cremation, the collagen cannot drag the bone mineral along. As a result, warping and transverse cracking in dry bone are minimal and of different kind.

In mechanical terms, the transverse cracks formed in a fleshed bone during cremation are perpendicular to the direction of the collagen tensile forces, as when wedging a log. This results in curved or serrated transverse fractures. In dry bone, where the tensile forces of the collagen are weak and the transverse forces predominate, the transverse cracks are the result of a "tearing" phenomenon; that is, the shearing forces are perpendicular to the direction of the crack. This results in straight transverse or step fractures that extend from the margin of the longitudinal fractures across the bone. Such a step fracture is shown in Fig. 5.

As can be observed from the long bones of the male skeleton, the preservation of the

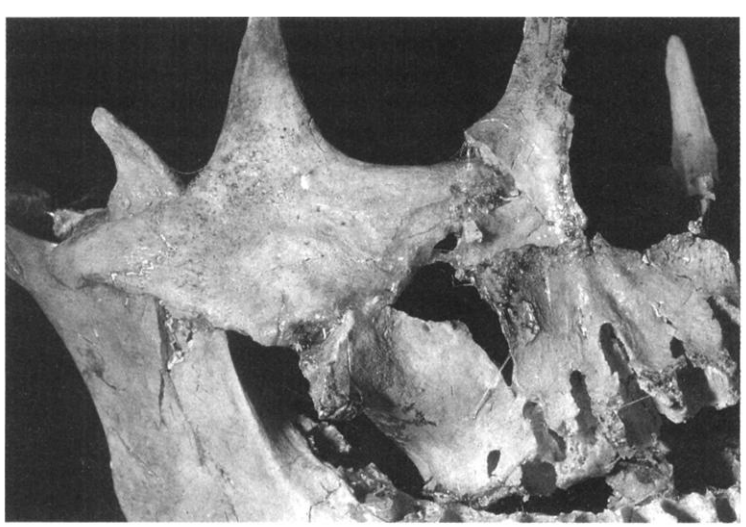

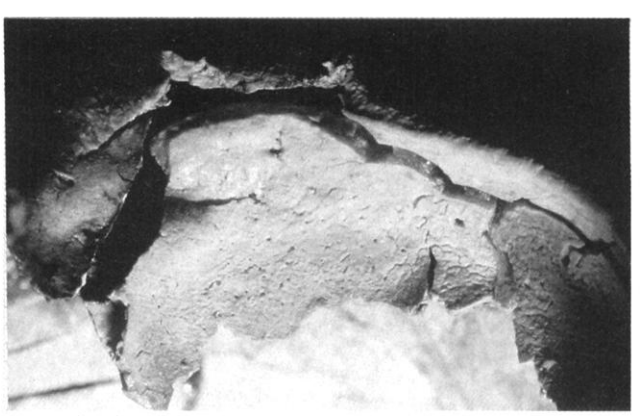

Fig. 3 (left). The area of zygomaticomaxillary suture showing the "nick," that is, the misalignment of bones owing to the fact that some fragments, such as the jugal crest shown here, are badly stuck together. No evidence of injury can be observed. **Fig. 4 (right).** The left orbital margin of the male occupant (internal view). The asymmetry observed between the two orbits (*6*) is mainly a postmortem effect: The top part of the bone was lifted up during cremation.

Fig. 5. The left tibia. A typical example of a long bone from the male skeleton: nearly intact, with minimal warping and a step transverse fracture, which are are all evidence of a dry bone cremation consistent with the taphonomic history of Arrhidaeus. Note that the step fracture in the distal part of the tibia extends from the end of the longitudinal crack across the shaft of the bone.

bones is excellent, with minimal warping and transverse cracking that is straight (Fig. 5). The skeleton is almost complete (*11*), and light brown is the dominant color of the bones. Only the left proximal ulna presents some curved transverse fractures, probably the result of insufficient decomposition in this area. The right ulna is nearly perfect, with a longitudinal crack. This type of preservation of the male skeleton shows that most of the bones were dry when cremated; that is, they were buried for some time before they were cremated. This is consistent with the taphonomic history of inhumation, cremation, and reinterment that only the bones of Arrhidaeus underwent, as already mentioned. Nevertheless, Musgrave reported that the bones appear sufficiently warped to have been burned fleshed (*11*), although he accepts the near-completeness and the huge size of many bones (*6*), the lack of transverse breaks, and the slight warping of many bones (*6*), despite his own experiments in a kiln with a dry radius that showed no transverse cracking (*13*). To explain the good preservation of these bones, he suggested a different cremation technique (*13*): burning in a brick box constructed around the body (*6*). But of course the real reason for the good preservation is the conspicuous lack of transverse cracks in many of the bones.

King Philip II suffered severe injuries, but there is no skeletal evidence whatsoever of any injuries to the male occupant of Royal Tomb II at Vergina, especially in the orbital bones. The reported facial injuries and asymmetries are mainly the result of cremation and poor reconstruction of the skull; there is thus strong anthropological evidence against a Philip II identification. The skeletal evidence that shows a dry bone cremation leaves no room for doubt that Royal Tomb II belongs to Philip III Arrhidaeus. This is consistent with the archaeological evidence that points to a later date (*2, 3*) for Royal Tomb II. In this case, some of the artefacts of Royal Tomb II may belong to Alexander the Great (*2*), which Philip III Arrhidaeus inherited from his half-brother Alexander in Babylon and brought back to Macedonia (*2*), where he was buried with them as the last king of the Argeads.

References and Notes

1. M. Andronicos, *Vergina: The Royal Tombs* (Ekdotike Athinon, Athens, Greece, 1994).
2. E. N. Borza, *Phoenix* **41**, 105 (1987); *In the Shadow of Olympus. The Emergence of Macedon* (Princeton Univ. Press, Princeton, NJ, 1992).
3. The archaeological evidence itself now weighs strongly in favor of a post–Philip II identification. In their recent work on the Derveni tombs, which date to the late 4th century B.C., P. Themelis and J. Touratsoglou [*The Derveni Tombs* (Publication 59, TAPA, Athens, Greece, 1997)] describe pottery similar to that in Tomb II at Vergina, thus moving the date of Vergina Royal Tomb II down to the generation after the death of Philip II. See also O. Palagia, *Minerva* **9**, 25 (1998). Palagia's views are expanded in her article "Hephaestion's Pyre and the Royal Hunt of Alexander," in *Alexander the Great: Fact and Fiction*, A. B. Bosworth and E. J. Baynham, Eds. (Oxford Univ. Press, Oxford, 2000).
4. N. I. Xirotiris and F. Langenscheidt, *Archaiologike Ephemeris* **1981**, 142 (1981).
5. A. S. Riginos, *J. Hell. Stud.* **114**, 103 (1994). It is not clear whether Philip II's left or right arm was maimed.
6. A. J. N. W. Prag, J. H. Musgrave, R. A. H. Neave, *J. Hell. Stud.* **104**, 60 (1984).
7. J. Prag and R. Neave, *Making Faces, Using Forensic and Archaeological Evidence* (British Museum Press, London, 1997), pp. 53–84.
8. A. J. N. W. Prag, *Am. J. Archaeol.* **94**, 237 (1990).
9. B. K. B. Berkovitz and B. J. Moxham, *Color Atlas of the Skull* (Mosby-Wolfe, London, 1989).
10. See, for example, T. D. White and P. A. Folkens, *Human Osteology* (Academic Press, San Diego, CA, 1991), fig. 4.2; G. Hauser and G. F. De Stefano, *Epigenetic Variants of the Human Skull* (E. Schweizerbartsche Verlagsbuchhandlung, Stuttgart, Germany, 1989), plate VIII.
11. J. H. Musgrave, in *Current Topics in Oral Biology*, S. J. Lisney and B. Matthews, Eds. (Univ. of Bristol Press, Bristol, UK, 1985), pp. 1–16.
12. N. Xirotiris, who did the reconstruction of the face, said on Greek television in 1999 that he was the one who misreconstructed the maxilla, that it was the best one could do at the time to preserve and support these delicate parts of the facial anatomy, and that it was probably this reconstruction that misled Musgrave. Indeed, the facial surgeons J. Lendrum and E. Curphey, who first suggested the antemortem asymmetry of the face (*7*), examined only the casts of the mandible and the maxilla. The consolidants and glues Xirotiris used are reversible.
13. J. Musgrave, *Annu. Br. Sch. Athens* **85**, 271 (1990).
14. W. L. Adams, *Ancient World* **22**, 27 (1991).
15. T. D. Stewart, *Essentials of Forensic Anthropology* (Thomas, Springfield, IL, 1979), pp. 59–68; D. H. Ubelaker, *Human Skeletal Remains* (Taraxacum, Washington, DC, 1991); N. P. Herrmann and J. L. Bennett, *J. Forensic Sci.* **44**, 461 (1999).
16. See, for example, P. Shipman, *Life History of a Fossil. An Introduction to Taphonomy and Paleoecology* (Harvard Univ. Press, Cambridge, MA, 1981).
17. D. W. Von Endt and D. J. Ortner, *J. Archaeol. Sci.* **11**, 247 (1984).
18. P. E. Hare, in *Fossils in the Making. Vertebrate Taphonomy and Paleoecology*, A. K. Behrensmeyer and A. P. Hill, Eds. (Univ. of Chicago Press, Chicago, IL, 1980), pp. 208–219.

19. I thank A. Kottaridou for allowing me to study the male skeleton of Royal Tomb II and M. Teliopoulou for curating it during the study.

11 November 1999; accepted 14 January 2000

Emergence of Genetic Instability in Children Treated for Leukemia

B. A. Finette,[1,2,3]* A. C. Homans,[1,3] R. J. Albertini[2,3,4]

T cells from patients who had received chemotherapy for B-lineage acute lymphocytic leukemia were studied to determine whether genetic instability, a principal characteristic of cancer cells, can also occur in nonmalignant cells. Consistent with expectations for a genetic instability phenotype, multiple mutations were detected in the hypoxanthine-guanine phosphoribosyltransferase (*HPRT*) reporter gene in independently isolated mutant T cells expressing identical rearranged T cell receptor β (TCRβ) gene hypervariable regions. These results indicate that cancer treatment can lead to genetic instability in nonmalignant cells in some individuals. They also suggest a mechanistic paradigm for the induction of second malignancies and drug resistance.

Carcinogenesis is a multistep process in which somatic cells acquire a series of stable genetic mutations in a specific clonal lineage. How multiple mutations accumulate in the same cell over a clinically relevant time period remains unclear, because individual spontaneous mutations ($\sim 1 \times 10^{-5}$ to 1×10^{-7} mutation per cell division) occur at low rates in vivo. One hypothesis states that genetic instability develops early to produce an increased rate of mutations in a distinct clone (*1*, *2*); another postulates that multiple mutations simply accumulate as a consequence of extensive clonal proliferation (*3*). In either case, genetic instability likely involves cellular changes that affect the expression and/or function of cell cycle (*4–6*), cell death (*7*), and DNA repair pathways (*8*). These cellular changes have been presumed to be unique to premalignant or frankly malignant cells. The purpose of this